COMPARISON BETWEEN DIRECT AND NON-INTRUSIVE MEASUREMENTS OF THE TEMPERATURE FIELDS IN RAYLEIGH BENARD CONVECTION

by

SYED ASAD HUSAIN

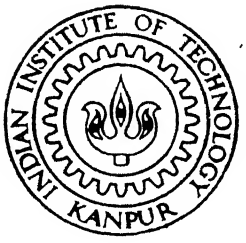

DEPARTMENT OF MECHANICAL ENGINEERING

INDIAN INSTITUTE OF TECHNOLOGY KANPUR

March, 1997

COMPARISON BETWEEN DIRECT AND NON - INTRUSIVE MEASUREMENTS OF THE TEMPERATURE FIELDS IN RAYLEIGH BENARD CONVECTION

A thesis submitted
in Partial Fulfillment of the Requirements
for the Degree of

M A S T E R O F T E C H N O L O G Y

by

SYED ASAD HUSAIN

to the
DEPARTMENT OF MECHANICAL ENGINEERING
INDIAN INSTITUTE OF TECHNOLOGY, KANPUR
MARCH, 1997.

CERTIFICATE

It is certified that the work contained in the thesis entitled **COMPARISON BETWEEN DIRECT AND NON-INTRUSIVE MEASUREMENTS OF THE TEMPERATURE FIELDS IN RAYLEIGH BENARD CONVECTION,** by **Syed Asad Husain,** has been carried out under our supervision and that this has not been submitted elsewhere for a degree.

(On leave)

(Dr. K. Muralidhar)
Dept. of Mechanical Engg.
Indian Institute of Technology
Kanpur 208 016, India

Gautam Biswas

(Dr. Gautam Biswas)
Dept. of Mechanical Engg.
Indian Institute of Technology
Kanpur 208 016, India

March, 1997.

ACKNOWLEDGEMENTS

I express my deep sense of gratitude to my guides Dr. G. Biswas and Dr K. Muralidhar for the guidance and encouragement throughout the thesis work.

I would like to express my thanks to Mr D. Mishra for all the help and cooperation extended to me.

I acknowledge the help extended to me by Mr. S.N. Sharma and Mr. B.P. Bhartiya for all the fabrication work needed in the thesis.

I thank all my friends who help and support me during various stages of my work.

Lastly, I would like to express my thanks to Mr S.K. Bhadra who helped me innumerable number of times throughout my thesis work. I express my sincere gratitude to my parents who have been a constant source of motivation to me.

Syed Asad Husain

CONTENTS

FIGURE	DESCRIPTION
1.1	Rayleigh Benard Convection.
1.2	Roll Formation in a Circular Cavity.
2.1	Schematic diagram of a Mach-Zehnder Interferometer.
2.2	Schematic diagram of a CCD camera.
2.3	Schematic diagram of a Traversing Mechanism for Direct Measurement.
2.4	Schematic diagram of the Test Cell.
2.5	Complete view of the Experimental Set Up with its Accessories.
2.6	Closer view of the Experimental Set Up.
2.7	Experimental Set Up with the Traversing Mechanism for Direct Measurement.
3.1	Schematic diagram for heat flux calculation
3.2	Schematic diagram for calculated of absolute fringe temperature
4.1	Geometry and Nomenclature for a plane in Axisymmetric Field.
5.1	Original Image with Intensity Variation. (a) 0^0 degree Projection. (b) 90^0 degree Projection.
5.2	Fourier Spectrum of the Original Image corresponding to the 0^0 degree Projection.
5.3	Filtered Image with Intensity Variation.

NOMENCLATURE

g	Acceleration due to gravity
h	Height of the cavity
k	Thermal conductivity of the fluid
L	Length of path of beam in the test cell
n	Refractive index
q	Heat flux at the wall
R	Radius of the test cell
Ra	Rayleigh number
T	Temperature
T_{ref}	Temperature of reference section in the interferometer
T_h	Temperature of hot surface
T_c	Temperature of cold surface
λ	Wavelength in the medium
λ_0	Wavelength in the vacuum
ε	Path difference per fringe shift
ρ	Density of the fluid
ΔT_ε	Temperature difference per fringe shift
ν	Kinematic viscosity
α	Thermal diffusivity
β	Thermal expansion coefficient

ABSTRACT

Steady state Rayleigh Benard Convection inside a circular cavity is studied by both non-intrusive and direct measurement methods for the Rayleigh number of 6872 and aspect ratio of 42.22. In non-intrusive method, Mach Zehnder Interferometer with a 35 mW He Ne laser source is used to produce the interferograms. The interferograms are recorded by CCD camera. The fringes of a interferogram are the locus of constant density or constant temperature lines. These interferograms are fourier filtered and thinned in order to obtain isotherms. The fringe temperatures are calculated by fitting a quadratic curve near the wall. The temperature data is then transferred onto a uniform grid using interpolation.

Two different projections are taken by rotating the test cell at angle $0^{o}$and 90^{o}. The fringe pattern in the two projections are found similar which implies that the rolls are axisymmetric. Therefore *Onion peeling* method is used to reconstruct the temperature field of the circular cavity.

Direct measurement has also been done to compare the temperature data with the previous results. Temperature inside the test cell is measured using chromel-alumel thermocouple along a radius in one horizontal plane.

CHAPTER -1

INTRODUCTION

1.1 RAYLEIGH BENARD PROBLEM :

Rayleigh Benard Convection is one of the important problems of fluid mechanics. This problem was first studied by H.Benard at the beginning of this century. Rayleigh studied the problem analytically. Research has been going on in this area to understand flow pattern, the mechanism of transition and turbulence.

Rayleigh Benard Problem involves natural convective flow in a fluid layer enclosed between two horizontal parallel plates at two different temperatures, as shown in Figure 1.1. The lower plate is maintained at a temperature higher than the upper plate. For small temperature difference, ΔT between the plates, there exists a rest condition. The heavier fluid rest on the top of lighter fluid. The density difference is not enough to overcome the viscous friction in the fluid. Heat transfer takes place due to pure conduction only. There exists a critical temperature difference $(\Delta T)_c$ above which convection will start. The fluid establishes hot rising regions and cold falling regions with horizontal motion at top and bottom surfaces to maintain continuity. The rising fluid looses heat when it gets near cold top surface and thus moves downward again. Similarly the cold down going fluid gets warmed when it approaches the hot plate and then rises again. Thus mechanism culminates in a roll pattern.

Rayleigh introduced a dimensionless parameter R_a called Rayleigh number that helps in determining the nature of the flow.

$$R_a = \frac{g\beta h^3 (\Delta T)}{\nu\alpha}$$

where h is the vertical spacing between the two plates.

$\Delta T = (T_h - T_c)$, is the adverse temperature gradient.

T_h and T_c are hot and cold surface temperature

g is acceleration due to gravity.

β is co-efficient of thermal expansion.

ν is viscous diffusivity

α is thermal diffusivity

For low Ra number there is no flow and the heat is transferred due to pure conduction only. Above the critical Rayleigh number, the convection starts and a stationary repeatable roll pattern is formed at steady state. Figure 1.2 shows the axisymmetric roll formation in circular cavity.

Rayleigh Benard Convection is a model for atmosphere convection. The atmosphere convection like winds, cyclone, storms and monsoon depend on buoyancy driven motion of air. Physically no surface maintains a constant temperature. The different latitudes of earth can be considered as isothermal plates. Thus Rayleigh Benard Convection is the simplest yet efficient model for atmosphere convection. Therefore the study of Rayleigh Benard convection is important in order to understand the circulation in atmosphere. Thus it may be useful in weather forecasting.

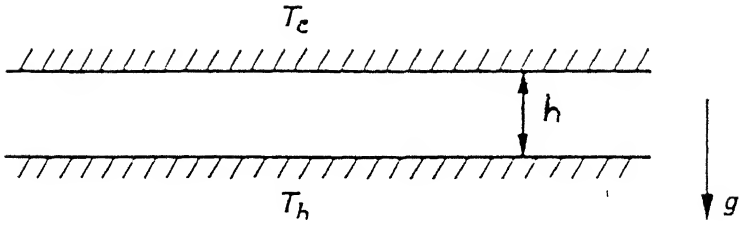

Fig 1.1 Rayleigh Benard Convection.

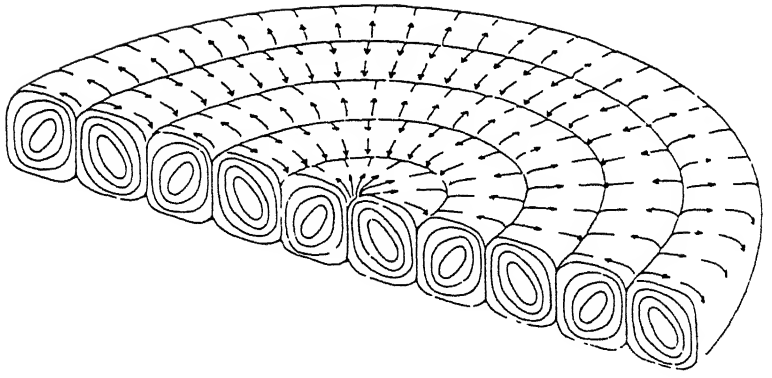

Fig 1.2 Roll Formation in a Circular Cavity.

1.2 LITERATURE SURVEY :

The Rayleigh Benard Convection problem has been studied over the past century by a large number of researchers. Rossby (1969) has described experimental study on stability of fluid in Rayleigh Benard convection with and without rotation of the test cell. Krishnamurti (1970) has presented a experimental study on the transition to turbulent convection in a Rayleigh Benard problem. Catton (1971) has studied theoretically the initiation of natural convection in fluid enclosed in a horizontal rectangle cavity.

Chu and Goldstein (1973) have studied turbulent convection in a horizontal layer of water for the Rayleigh Benard problem. In this study, Mach Zehnder interferometer with He Ne laser source was utilized to measure the mean temperature distribution for Rayleigh number between 10^5 to 10^8. The heat transfer mechanism was qualitatively studied by direct and photographic observation of the interferograms. Busse and Clever (1979) have described theoretically as well as experimentally the mechanism of instability of convection rolls in fluid of moderate Prandtl number. Shadowgraph visualization method has been used to study instability mechanism. Kim and Viskanta (1984) has studied experimentally and numerically the effect of wall conductance on natural convection in a differently oriented square cavity. Mach Zehnder interferometer with He Ne laser was used to determine the temperature distribution in fluid. Curry et al (1984) has done numerical and experimental study of 3-D cellular convection in a

rectangular cavity. Optical measuring techniques were used to study the various steady and time dependent convection processes. Arroyo and Saviron (1992) have studied experimentally the spatial features and thermal dependence of velocity field in a small box. Particle image velocimeter with He Ne laser as a source was used to measure velocity field in the mid plane of the cell.

Michael and Yang (1992) have studied the steady state Rayleigh number for a rectangle cavity. Mach Zehnder interferometer was used for data collection. The temperature field was reconstructed using ART algorithm. Forbes (1996) has described a numerical method for inversion of axisymmetric interferograms. The method is of ***Onion peeling*** type which can be used to invert the integrated phase shift data obtained from axisymmetric refractive index field.

CHAPTER-2

APPARATUS AND INSTRUMENTATION

2.1 INTRODUCTION :

Optical methods have been used in many engineering applications. Optical methods like schlieren, shadowgraph and interferometry are used to study density or temperature field in transparent medium. Interferometry is useful in study of those problem which involve small variations in the refractive index. Therefore Mach Zehnder interferometer has been used to study the temperature variation in the Rayleigh Benard convection problem. It is a non-intrusive and non-destructive method of measurement.

In order to validate our results, we have also accomplished the direct measurement. A thermocouple is put inside the test cell to measure temperature at few points. Arrangements are made such that the flow field gets least disturbed.

2.2 INSTRUMENTATION :

2.2.1 He-Ne LASER :

A 35mW He Ne laser (mode 127, spectra physics) is used as an optical source in Mach Zehnder interferometry. The wavelength of laser is 6328 Å which lies in visible region. The properties of He Ne laser are high degree of mono chromaticity and large coherence length. The He Ne laser is neutral gas laser with Ne atoms as active material. He atoms are useful in the excitation or pumping of Ne atoms. A small spot size light comes

out of laser which is expanded using beam expander. The expanded beam is collimated using a lens. The collimated beam is made incident on the Mach Zehnder interferometry.

2.2.2 MACH ZEHNDER INTERFEROMETRY :

Principle of Interferometry

The Mach Zehnder Interferometer works on the principle of interference of light. Two light beams originating from same coherent monochromatic source get superimposed. The optical path length along beam is defined by

$$PL = \int n \, dz$$

where n is the refractive index of the medium and

z is the direction along light beam.

The optical path difference between the two light beams, say beam 1 and beam 2 is given by

$$\Delta PL = PL_1 - PL_2$$

$$\Delta PL = \int_1 n \, dz - \int_2 n \, dz$$

$$= \lambda_0 \left[\int_1 \frac{dz}{\lambda} - \int_2 \frac{dz}{\lambda} \right]$$

where λ_1 and λ_2 are the wavelengths of light in path 1 and path 2 respectively. The corresponding phase change between the two beams is

$$\phi = \left(\frac{2\pi}{\lambda_0} \right) \Delta PL$$

$$= 2\pi \left[\int_1 \frac{dz}{\lambda} - \int_2 \frac{dz}{\lambda} \right]$$

Now let us take the equation of propagation of light beam 1 and beam 2 as

$$E_1 = A \sin \left(\frac{2\pi}{\lambda} x - \omega t \right)$$

$$E_2 = A \sin \left(\frac{2\pi}{\lambda} x - \omega t + \phi \right)$$

After superimposition of beam 1 and beam 2 we get

$$E = E_1 + E_2$$
$$= A \sin \left(\frac{2\pi x}{\lambda} - \omega t \right) + A \sin \left(\frac{2\pi x}{\lambda} - \omega t + \phi \right)$$
$$= 2A \cos\frac{\phi}{2} \sin \left(\frac{2\pi}{\lambda} x - \omega t + \frac{\phi}{2} \right)$$

So, the intensity of interference, $I = 4A^2 \cos^2\frac{\phi}{2}$ which says that the intensity varies as cosine square curve.

When $\phi = 2K\pi$ where K=0,1,2,3,.....

The interference is constructive and hence field is bright.

When $\phi = (2K - 1)\pi$ where K=1,2,3,.....

The interference is destructive and field will be dark.

Hence we get a interference pattern consists of dark and bright regions.

Description

The schematic diagram of Mach Zehnder Interferometer is shown in Figure (2.1). It consists of two mirrors M_1 and M_2 and two beam splitters BS_1 and BS_2. The mirrors and the beam splitters, M_1, M_2, BS_1 and BS_2 are inclined at angle of 45^0 with

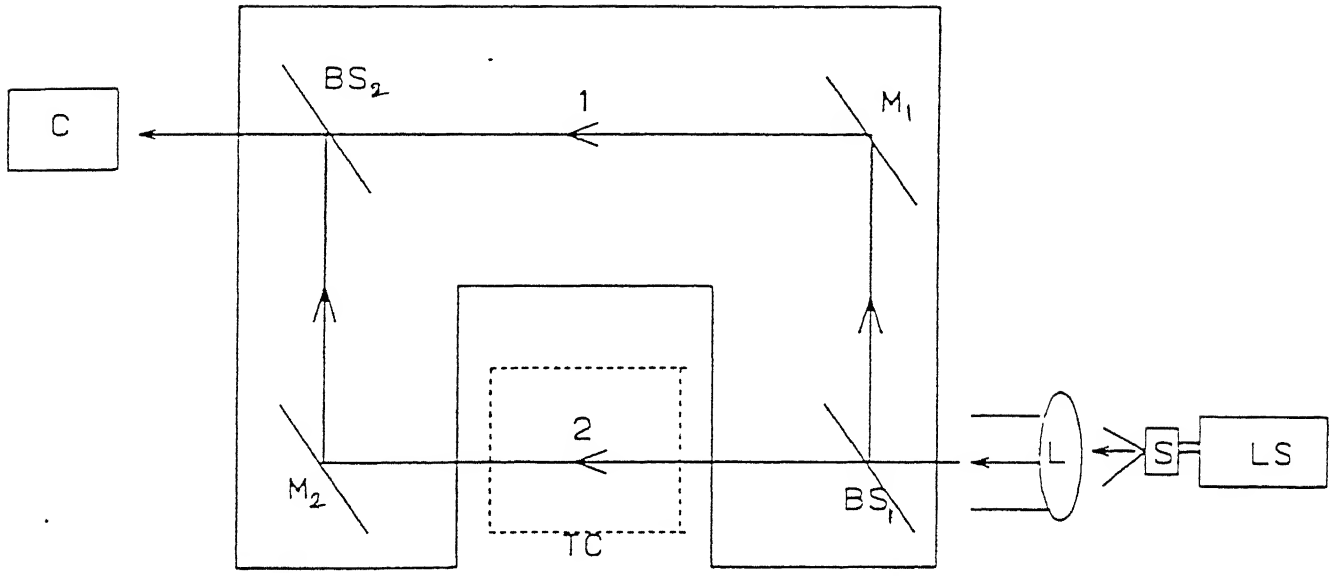

(a)

BS	Beam splitter	C	Camera
L	Convex lens	LS	He-Ne laser
M	Mirror	S	Spatial filter
1	Reference beam	2	Test beam

Fig 2.1 Schematic diagram of a Mach-Zehnder Interferometer.

the beam direction. The beam splitter BS_1 splits the incoming collimated beam into two equal parts beam 1 and beam 2. Beam splitter is a semi polished mirror which allows 50% light beam to transmit and reflects the rest 50% of light beam. The transmitted beam, i.e. beam 2 passes through test section and gets reflected by mirror M_2. Beam 1 gets reflected by mirror M_1 and passes through reference section. Beam 1 and beam 2 get superimposed at the beam splitter $BS_2$and form interference pattern.

Fringe pattern arising in a Mach Zehnder Interferometer

In Mach Zehnder interferometer beam 1 and beam 2 pass through test and reference section respectively. The path difference between beam 1 and beam 2 is given by

$$\Delta PL = \int (n - n_r) \, dz$$

where n & n_r are the refractive index of test and reference section.

Let $\varepsilon = \frac{\Delta PL}{\lambda_0} = \frac{1}{\lambda_0} \int (n - n_r) \, dz$

when ε is zero or an integer, we have constructive interference. If ε is not an integer then we have destructive interference. This forms a fringe pattern. Each fringe represents a particular value of ε. Adjacent dark or bright fringe differ by a value of ε =1.

Gladstone-Dale equation gives the relation of refractive index n with density ρ for any gas as given below

$$\frac{n-1}{\rho} = C$$

$$\frac{n-1}{\rho} = C$$

where C is constant.

$$\varepsilon = \frac{C}{\lambda} \int (\rho - \rho_0) \, dz$$

When temperature variation is small (upto 20^0), The density can be taken as linear function of temperature.

$$\frac{d\rho}{dT} = \text{constant}$$

Therefore $$\varepsilon = \frac{1}{\lambda_0} \int \left(\frac{dn}{dT} \right) (T - T_{ref}) \, dz$$

$$\varepsilon = \frac{1}{\lambda_0} \left(\frac{dn}{dT} \right) \int (T - T_{ref}) \, dz$$

$$\varepsilon = \frac{1}{\lambda_0} \left(\frac{dn}{dT} \right) (T - T_{ref}) \, L$$

Where T= mean temperature along z direction in test section.

T_{ref}= temperature of reference section

L = length of test section along beam direction

λ_0 = wavelength of light in vacuum

$\frac{dn}{dT} = 0.927 \times 10^{-6}$ per ^0C for air

$$T - T_{ref} = \left(\frac{\varepsilon \lambda_0}{L} \right) \left[\frac{1}{\left(\frac{dn}{dT}\right)} \right]$$

$$(T - T_{ref}) \propto \varepsilon$$

Hence each fringe is a locus of points where temperature is constant. In other words fringes correspond to isotherms.

Temperature difference for one fringe shift is given by

$$\Delta T_{\varepsilon} = \left[\frac{\lambda_o}{\left(\frac{dn}{dT} \right)_L} \right]$$

The above analysis is valid only when beam 1 and beam 2 are recombined parallel to each other. This setting is called infinite fringe setting.

2.2.3 CCD CAMERA :

A CCD (charge coupled device) camera is used to scanned the interference pattern formed in the Mach Zehnder Interferometer. The schematic diagram of a CCD camera is shown in Figure (2.2). Light intensity produces charges in the photosensor elements. These charges are transferred at the end of each integration period to adjacent vertical shift registers. The contents of each vertical shift registers are then transferred to horizontal shift register. Each transfer from vertical registers fills the horizontal register which produce a video frame. After all lines are read out the process starts again. The image is stored as an array of 512 × 512 pixels. Each pixel is assigned a value between 0 to 255 depending on the intensity level. The image is stored on the hard-disk of a PC.

2.2.4 DIRECT MEASUREMENT :

Thermocouple

Chromel Alumel thermocouple is used to measure the

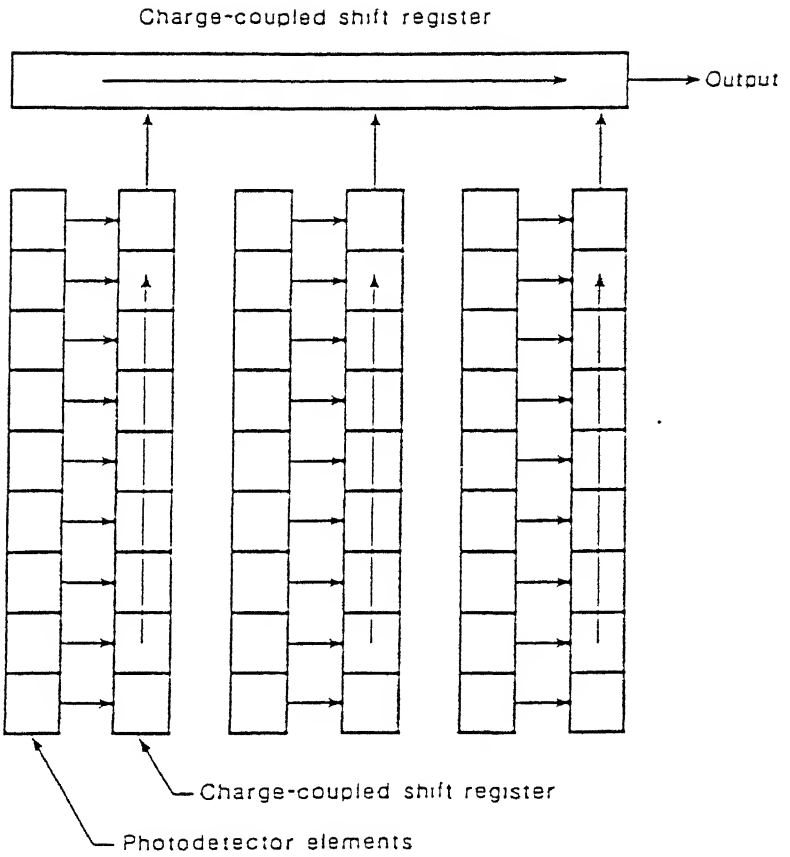

Fig 2.2 Schematic diagram of a CCD camera.

-200°C to 1300°C. It gives ± 5°C (0 to 350°C) and ± 0.75% (350 to 1300°C) accuracy. Thermocouple works on principle called Seeback effect. If two junctions of two dissimilar metals, are maintained at different temperatures, then a break anywhere in the circuit will give an emf called as thermoemf. Thus thermocouple produce a voltage difference. The thermocouple performance is affected by the heating of junctions between dissimilar materials when a current flows through them. This is known as Peltier effect. The thermocouple performance also depends on Thomson effect which is related to an emf production due to temperature gradient along the length of wire. These give an error in thermocouple measurement. The errors can be kept small by using shorter length of the thermocouple wires and using high conductivity copper wire to convey the thermoemf to the measuring instrument, i.e., to the Hybrid Temperature Recorder.

Hybrid Temperature Recorder

A 8H10 hybrid temperature recorder has been used to measure the temperatures using thermocouple. The recorder has a capacity of taking input data from 30 channels simultaneously. It displays the measured value from each channel at approximately 4 seconds interval. It can also be used for various combination of thermocouples over a wide range of temperature. Internal compensation is built-in as a reference junction.

Traversing Mechanism

The schematic diagram of traversing mechanism is shown in Figure 2.3. Thermocouple wires are kept inside a thin glass tube of diameter (5 mm). The glass tube is then passed through three holes made in perspex sheets as shown in the diagram. The holes are in horizontal line. Therefore glass rod can only be moved in horizontal direction. The distance traversed by rod is measured by the scale fixed in the mechanism.

2.3 FABRICATION OF TEST CELL :

The test cell used to study Rayleigh Benard Convection Problem is shown in Figure 2.4. It consists of a top tank, a bottom tank and a cavity filled with the working fluid.

The cavity is of circular cross section with its diameter 76 cm and height 1.8 cm. The top and the bottom walls of the cavity are made of aluminium sheet. The side wall is made of a perspex ring of height 1.8 cm. Two windows of width 5.7 cm are made in perspex ring along beam direction. Foam is used around the side wall as an insulator.

The top tank is made up of aluminium sheet and a perspex ring. The perspex ring is fixed with the aluminium sheet with the help of araldite and M-seal. Aluminium sheet is used as the base plate because of its high thermal conductivity. It gives uniform temperature throughout the top surface of cavity.

The bottom tank is also made up of aluminium sheets. The top and bottom surfaces are made of aluminium sheets and the

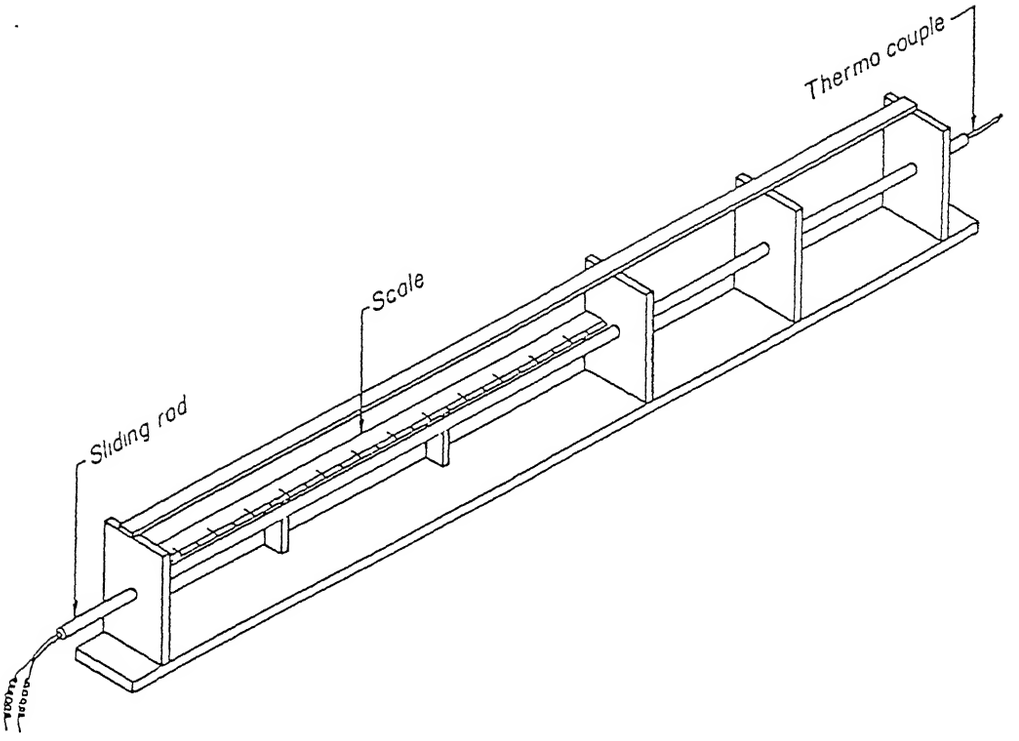

Fig 2.3 Schematic diagram of a Traversing Mechanism for Direct Measurement.

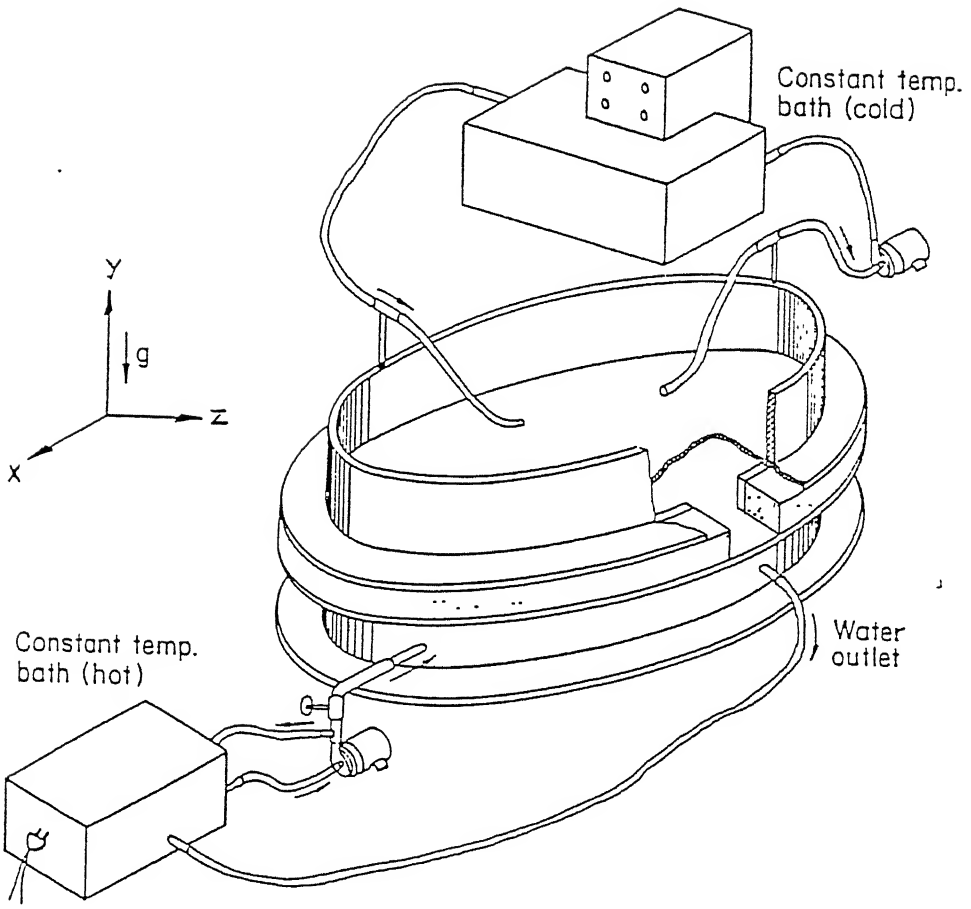

Fig 2.4 Schematic diagram of the Test Cell.

side wall of the tank is made of aluminium ring. The sheets are fixed to the ring with the help of screws. All the joining lines are sealed using araldite and M-seal. Three baffles are fixed inside the tank at equal intervals to control and direct the flow inside the tank.

The hot water bath supplies hot water to the bottom tank. The water is heated up in a separate tank with the help of 1 kW heater. Power supply to the heater is given through a variac. The hot water is pumped to bottom tank with the help of a Tullu Pump. The water flow rate is controlled by a valve. Excess water is flowed back to the heating tank. Water is drained back from bottom tank with the help of tubing arrangement. The temperature of water is controlled by changing voltage supply to the heater.

Variostat supplies constant temperature cold water to the top tank. It has a operating range between $-30^{o}C$ and $150^{o}C$. It consists of a heating element, an air cooled refrigerating unit, a forced pump and a suction pump. Cold water is pumped to the top tank and drained back with the help of suction pump.

2.4 REPEATABILITY OF THE SET UP :

The flatness of top and bottom wall of the cavity is one of the requirement for the Rayleigh Benard Convection Problem. At steady state the temperature variation over the two wall is within $\pm 0.2^{o}C$. The top and bottom tank are kept horizontal. During the experiment, the windows are kept closed

with foam in order to avoid circulation of air between the atmosphere and the cavity. The interferometer is aligned to infinite fringe setting. In this setting the fringes are isotherms. The whole experiment takes about 8 hours to get the steady roll pattern. If the interferometer is aligned properly and the experiment is run for sufficient long time, we get repeatability.

Fig 2.5 Complete view of the Experimental Set Up with its Accessories.

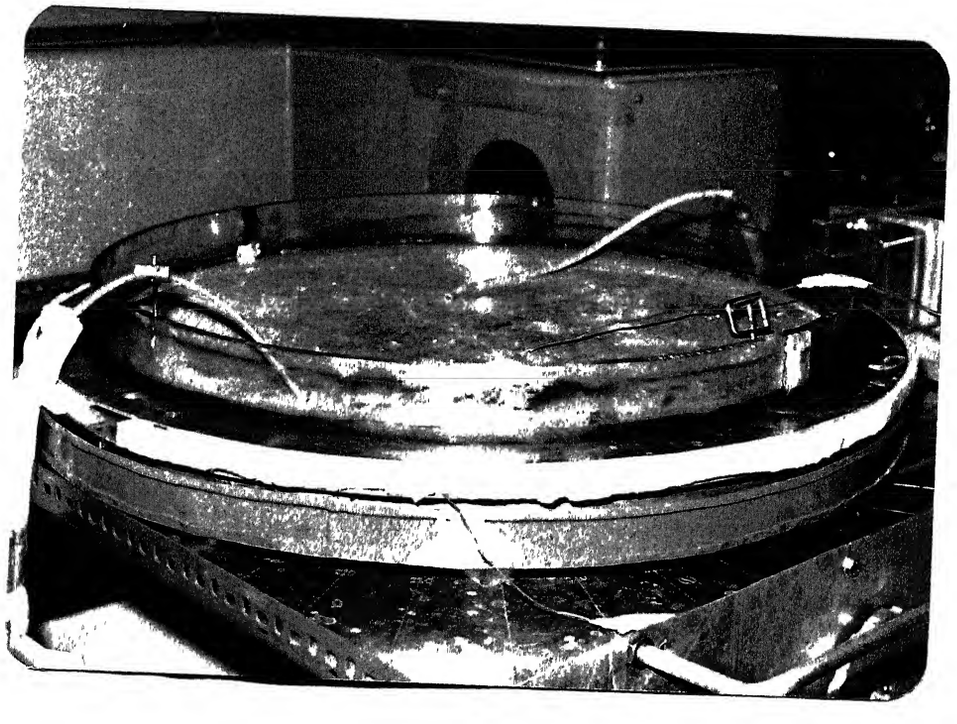

Fig 2.6 Closer view of the Experimental Set Up.

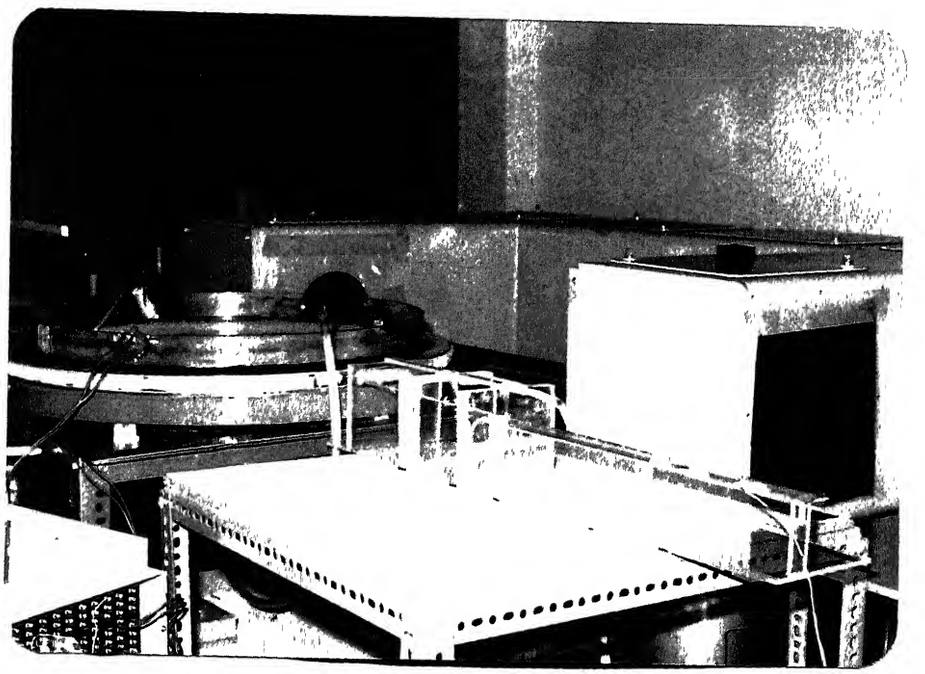

Fig (2.7) Experimental Set Up with Traversing Mechanism for Direct Measurement.

CHAPTER-3

EXPERIMENTAL PROCEDURE AND DATA REDUCTION

3.1 INTRODUCTION :

The Rayleigh Benard Convection is a sensitive experiment. All the experiments are done only for one Rayleigh Number, Ra=6872 which lies in the range of roll formation. The data is recorded only when steady state condition is reached.

In non-intrusive method the images are recorded by Mach Zehnder interferometer. These images are needed to be cleaned and thinned. The temperature data is obtained from thinned image using certain mathematical techniques.

In direct measurement, temperatures are recorded by putting one thermocouple inside the test cell using traversing mechanism. Temperatures are recorded at different radii along a line in one horizontal plane.

3.1.1 OVERVIEW OF THE PROCEDURE :

The pneumatic legs of Mach Zehnder interferometry are pressurized to about 2 bar such that no external vibration can disturb the infinite fringe setting. Initially there is no thermal disturbance in the test section. Hence we expect a bright interferogram. Mirror M_2 or beam splitter BS_2 are adjusted such that we get a bright interferogram. This is known as infinite fringe setting. The test cell is now placed in the path of test beam. The light beam enters through the window and passes through the center of the cavity. The hot water is pumped to the bottom

tank and cold water is flowed to the top tank. It requires about 4 hours to reach a steady state temperature for the top and the bottom surfaces of the cavity. The top and bottom surfaces are maintained at 22.5^{0}C and 35.5^{0}C respectively. The corresponding value of Rayleigh number is 6872 which lies in the ranges where rolls are formed. Another 3 hours is needed for the flow to reach steady state condition. The image is recorded in a PC. Images are taken at two different angles 0^{0} and 90^{0} by rotating the test cell.

3.1.2 DIRECT MEASUREMENT OF TEMPERATURE :

Initially the probe is adjusted to be at the center of the cavity ie. radius=0. and at a height 1 cm above the bottom surface. Temperatures are recorded only when the flow become steady for the same Rayleigh number. The temperatures are recorded at a radial distance of 2 mm. Considerable time is given for the flow to become steady. The probe is moved along the radius in a horizontal plane 1 cm above from bottom surface of the test cell. The temperature readings are taken at 28 points in a gap of 2 mm starting from center of the cavity.

3.2 DATA REDUCTION :

Interferometric fringes are processed to get thin fringes. Processing of image involves fourier filtering, contrast improvement, edge detection and thinning.

. In fourier filtering, the noise of the image is removed. The noise is unwanted data that arises due to optical system. Speckle is the information about microscopic variation or

unevenness of the optical surfaces. The fluid near the cavity is affected by ambience. This also induces noise. The noise is characterized by high frequency fluctuations in the intensity data of the image.

The fringes are broad band. The minimum intensity line of each fringe represents the skeleton of the fringe. Each skeleton is a constant phase line or a constant temperature line.

Using certain mathematical techniques the absolute temperatures of skeleton are determined.

3.2.1 FILTERING OF THE IMAGES :

Fourier filtering requires the use of two dimensional fast fourier transform which helps in moving the image to the frequency domain. speckle noise is characterized by the high frequency components. The high frequency domain is cut off using a 2-D symmetric band pass filter. The 2-D inverse fast fourier transform is carried out to get a filtered image.

Thus the fourier filtering of interferometric fringes has been carried out with the following steps :-

1) 2-D fast fourier transform
2) 2-D filtering
3) 2-D inverse fast fourier transform

The image is stored in an array of 512x512 pixels where each pixel value is an intensity level. The discrete fourier transform in one dimension is given by :-

$$F(u) = \frac{1}{N} \sum_{x=0}^{N-1} f(x) \exp \left[-i2\pi ux/N \right] \qquad (3.1)$$

where u = 0,1,2,.....N-1, and N is the size of image. In present study, N is 512.

Here the number of multiplication and addition required is proportional to N^2. But fast fourier transform require N $\log_2 N$ multiplications only. Therefore fast fourier transform takes less computational time. This algorithm works on the image whose data size is of power of 2.

FFT algorithm is based on method of successive doubling method. The equation (3.1) can be expressed as

$$F(u) = \frac{1}{N} \sum_{x=0}^{N-1} f(x) \, W_N^{ux} \qquad (3.2)$$

where u= 0,1,2, ...N

and $W_N = \exp \left[-i2\pi/N \right]$

N should be of the form $N = 2^n$. Where n is any integer. Also N is such that it can be expressed as N = 2M, M being any other integer. The expression (3.2) can be decomposed into following two parts,

$$F(u) = \frac{1}{2} \left[F_{even}(u) + F_{odd}(u) \, W_{2M}^{u} \right] \qquad (3.3)$$

where, u = 0,1,2,.....(M-1)

$$\text{and } F(u + M) = \frac{1}{2} \left[F_{even}(u) - F_{odd}(u) \, W_{2M}^{u} \right] \qquad (3.4)$$

where, u = 0,1,2, ...(M-1)

The expression for $F_{even}(u)$ and $F_{odd}(u)$ are given by,

$$F_{even}(u) = \frac{1}{M} \sum_{x=0}^{M-1} f(2x)\ W_M^{ux} \tag{3.5}$$

$$\text{and } F_{odd}(u) = \frac{1}{M} \sum_{x=0}^{M-1} f(2x+1)\ W_M^{ux} \tag{3.6}$$

Evaluation of the first half of F(u) (given by equation (3.3)) requires calculation of two $(\frac{N}{2})$ single point transformation. The resulting values of $F_{even}(u)$ and $F_{odd}(u)$ are used in equation (3.4) to evaluate the other half of F(u). The total number of operation requires is $N \log_2 N$. In the present analysis, 2-D FFT has been used for a full image. 1-D FFT has been done in two directions, ie., first along each row and then along each column. The total number of operations required for the 2-D FFT is $2N^2 \log_2 N$.

Inverse FFT can also be formulated in the same way. The discrete form of inverse fourier transform is given by:

$$f(x) = \sum_{u=0}^{N-1} F(u)\ \exp\left[\ i2\pi ux\ /\ N\ \right] \tag{3.7}$$

3.2.2 THINNING OF THE FILTERED IMAGE :

In fringe thinning, the band of dark fringes are replaced by fringe skeletons. A fringe skeleton is the minimum intensity line or the locus of mid point of the fringe band. The

image become blurred due to the removal of high frequencies in fourier filtering. Therefore contrast improvement of the filtered image is required. This is done by Histogram Equalization of the image using KIP software. This helps in improving the image contrast and appearance. Then the edge detection of the fringes is done by setting a pointer along the edge of a fringe band and recording the co-ordinates of the points. The line joining these points represent the edge of the fringe. The mid points of the fringe is calculated. The curve fitted through the mid points represent the fringe skeleton or thinned fringe. Each fringe skeleton is a constant temperature line.

3.2.3 DETERMINATION OF FRINGE TEMPERATURE :

The fringes are constant temperature lines. But the temperature of the fringes are unknown. Top and bottom surface temperature and the temperature difference per fringe shift are known quantities. First we determine the heat flux near any wall. This can be accomplished in the following way,

Let $T(y) = a + by + cy^2$

where, a,b and c are three unknowns.

Let us take three fringes near the wall as shown in Figure (3.1). Let Y_0, Y_1, Y_2 and Y_3 be the distances of the wall, the first, the second and the third fringe measured with respect to the first fringe. T_1, T_2 and T_3 are temperatures of the three fringes respectively. Now it can be possible to write the following,

$Y_1 = 0$

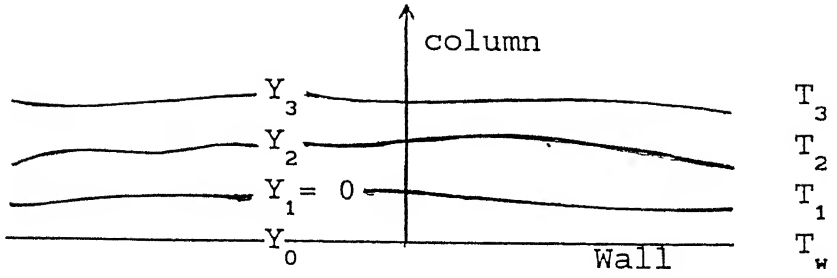

Fig.3.1 Schematic Diagram for Heat Flux Calculation.

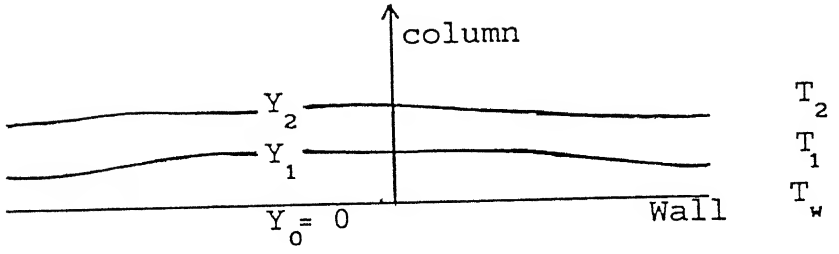

Fig.3.2 Schematic Diagram for Calculation of Absolute Fringe Temperature.

$$T_1 = a$$

$$T_2 = a + by_2 + cy_2^2$$

$$T_3 = a + by_3 + cy_3^2$$

Solving the above equations we get

$$b = \frac{(y_3^2 - 2y_2^2)\,\Delta T_\varepsilon}{y_2 y_3 (y_3 - y_2)}$$

$$c = \frac{(2y_2 - y_3)\,\Delta T_\varepsilon}{y_2 y_3 (y_3 - y_2)}$$

Where ΔT_ε is the temperature difference per fringe and given by expression

$$\Delta T_\varepsilon = \left[\frac{\lambda_0}{\frac{dn}{dT} L}\right]$$

Hence wall heat flux can be calculated as

$$q_w = -k\frac{\partial T}{\partial y}\Big|_{y=y_0} = -k(b + 2cy_0)$$

where, k is thermal conductivity of the fluid.

Now we determine the temperature of the first fringe, T_1 Again fit a quadratic curve near the wall.

$$T(y) = A + By + Cy^2$$

where, A,B and C are unknowns. Let us take two fringes near wall as shown in Figure (3.2). Let y_1, y_2 and y_0 are distances of first first, the second fringe and the wall measured with respect to the wall. Also T_1, T_2 and T_w are the corresponding temperatures. Now it is possible to write the following,

$$y_0 = 0$$

$$T_w = A$$

$$T_1 = A + By_1 + Cy_1^2$$

$$T_2 = A + By_2 + Cy_2^2$$

$$\left.\frac{\partial T}{\partial y}\right|_{y=y_0} = -\frac{q_w}{K} = B$$

Solving the above equations

$$C = \frac{\Delta T_\varepsilon + B(y_1 - y_2)}{(y_1^2 - y_2^2)}$$

Once B and C are known, T_1 can be calculated using, $T_1 = A + By_1 + Cy_1^2$. If T_1 is known, the temperatures of all other fringes are determined following the following relationships,.

$$T_2 = T_1 \pm \Delta T_\varepsilon$$

$$T_3 = T_1 \pm \Delta T_\varepsilon$$

and so on.

The positive (+) or negative (-) signs are used for the calculations from the cold or the hot walls respectively.

3.3 TRANSFERRING DATA ON TO A GRID :

A uniform grid (typically 21×21) is placed on the image. The temperature of the grid points are required to found out. The temperature of the points lying on the fringes are known. A cubic spline curve is fitted along a column using known temperature points. The temperature of the grid points along that

column is determined from the fitted curve. The same procedure is done for all columns of the grid. Thus we get the temperature of all points on the grid.

3.4 RECORDING TEMPERATURE AT DIFFERENT RADII :

The non dimensional temperature versus distance is plotted. Temperature and corresponding position of probe are non dimensionalised in the following way,

$$T_{non} = \frac{(T - T_m)}{(T_h - T_c)}$$

$$r_{non} = \frac{r}{h}$$

where, T_m is the mean temperature. T_h and T_c are hot and cold surface temperatures respectively, r is radial distance and h is the height of the cavity.

CHAPTER - 4

IMAGE RECONSTRUCTION FROM PROJECTION

4.1 INTRODUCTION :

The method for image reconstruction from a projection is discussed in this chapter. ***Onion Peeling method*** is used for mathematical formulation because of axisymmetric roll formation. Special ART algorithm is used for reconstruction the temperature field.

4.2 MATHEMATICAL FORMULATION :

Let (r,θ,y) be the co-ordinates of the circular cavity with its origin at the center of the cavity. The plane $y = +0.9$ and $y = -0.9$ are the top and bottom surface respectively. Due to axisymmetric roll formation in the circular cavity, temperature can be considered as the function of r and y only. The projection data or the grid data is on x-y plane. The grid data is available from $x = 2.85$ to $x = -2.85$. Due to symmetrical geometry with respect to z axis, only one half of the grid data is used at a time for reconstruction. The temperature on grid is mean temperature along a ray direction, i.e., z direction.

$$\int_0^L T \, dz = C \times d \qquad (4.1)$$

Reconstruction is performed at one x-z plane at a time (constant y plane). Let temperatures at N circular rings are to

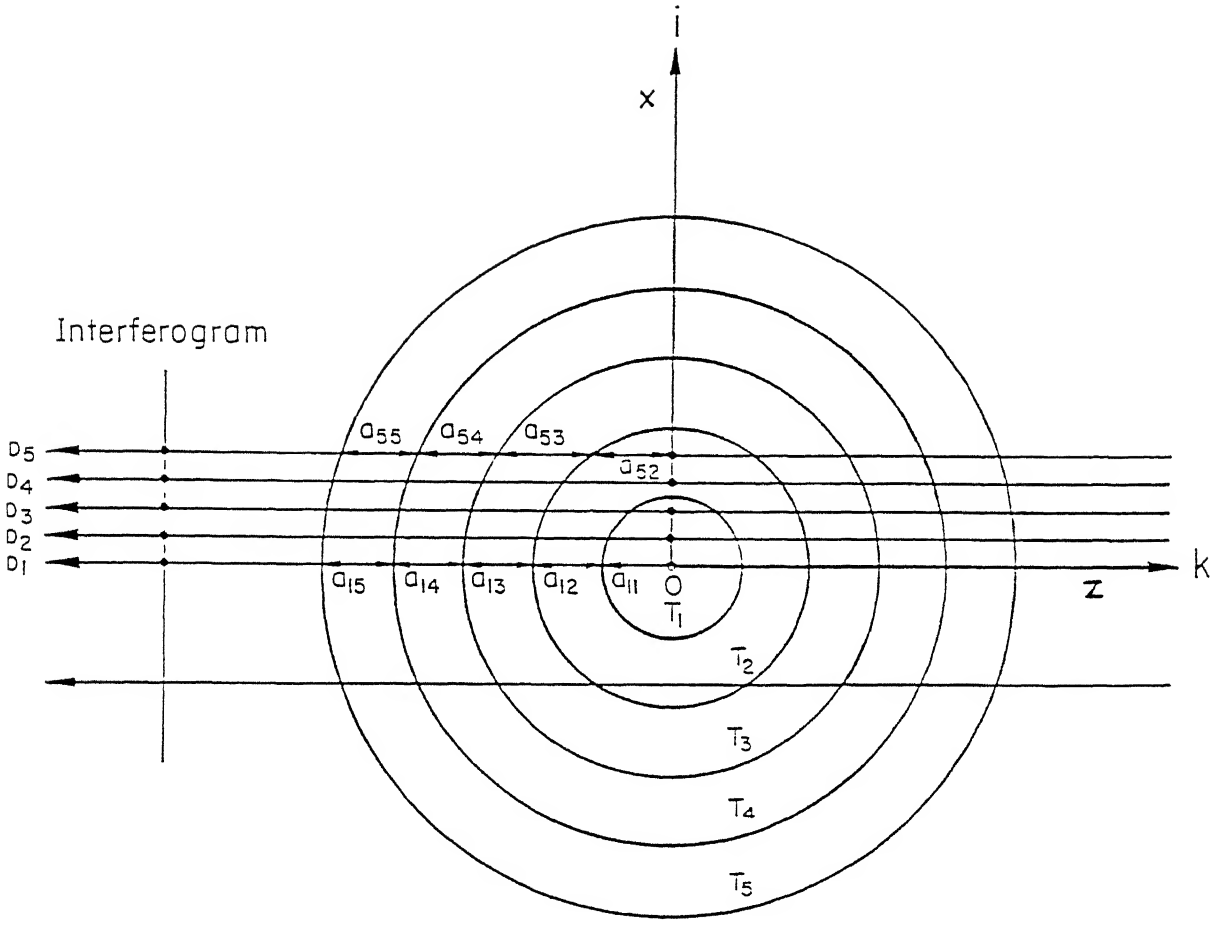

Fig 4.1 Geometry and Nomenclature for a plane in Axisymmetric Field.

be reconstructed. The circle of diameter 76 cm is divided into N uniformly spaced rings as shown in Fig (4.1). Each ring is at a constant temperature. The one half of the grid data is divided into N equal parts. The integral equation (4.1) for each ray can be discritized as given below,

$$\sum_{k=1}^{N} A_{ik}\, T_k = \frac{1}{2}\, C_i \times d_i \qquad (4.2)$$

where i = 1,2,3,4,.....,N.

A_{ik} is distance traversed by i^{th} ray in k^{th} ring.

d_i is mean temperature from projection data for i^{th} ray.

C_i is chord length for i^{th} ray.

T_k is reconstructed temperature for K^{th}ring in a particular y plane.

Let $D_i = \frac{1}{2}\, C_i \times d_i$

The equation (4.2) can be written a matrix form given below,

$$[\,A\,]_{N,N} \left\{ T \right\}_{N,1} = \left\{ D \right\}_{N,1}$$

where $[\,A\,]$ is geometric matrix.

$\left\{ D \right\}$ is projection matrix.

$\left\{ T \right\}$ is reconstructed temperature matrix.

4.3 SPECIAL ART ALGORITHM :

The SART (Special Algebraic Reconstruction Technique) is used to determine the reconstructed temperatures. The complete algorithm of ART is given below,

(1) Assume for ray i=1;

$T_k = T_k^0$ (initial guess)

(2) Do for ray i,

(a) Compute projection numerically $\tilde{D}_i$

(b) Compute the correction ($D_i - \tilde{D}_i$)

(c) Compute total value of weight function,

$$W = \sum_{k=1}^{N} A_{ik}^2$$

(d) Update each temperatures,

$T_k^{new} = T_k^{old} + \mu \; (D_i - \tilde{D}_i) \; A_{ik} \; / \; W$

where μ is the relaxation parameter.

(3) repeat step (2) for i=i+1, till i ≤ N

(4) store the temperatures,

$T_k^n = T_k^{new}$

(5) set n = n + 1 and i = 1;

go to step (2)

(6) Check for convergence in T_k^n

(7) repeat step (2) to (4) till convergence.

CHAPTER-5

RESULTS AND DISCUSSIONS

5.1 NON INTRUSIVE MEASUREMENT :

5.1.1 Qualitative Study :

Interferograms are recorded by passing the laser beam through 5.7 cm window along the diameter of test cell. Figure 5.1 shows the interferogram at 0^0 and 90^0. The number of fringe in each interferogram is 13. The fringe pattern in each of the interferograms is almost similar in nature. This indicates that the rolls are axisymmetric.

5.1.2 Data Extraction :

Interferograms are recorded at infinite fringe setting. Therefore fringes are constant phase lines or a constant temperature lines. Figure 5.1 shows the original interferograms with intensity variation along a column of the image. There are fluctuations in intensity due to the presence of noise. Noise is characterized by high frequency component in the fourier curve. Figure 5.2 shows the variation F(u) versus u_x for the original interferograms. The high frequencies are cut off from 80 in the frequency domain. Figure 5.3 shows the filtered images with intensity variation along a column. The intensity variation is smoother than that of original images. Due to removal of high frequencies, the image gets blurred. Histogram equalization is done in order to improve contrast of the image. Figures 5.4 and

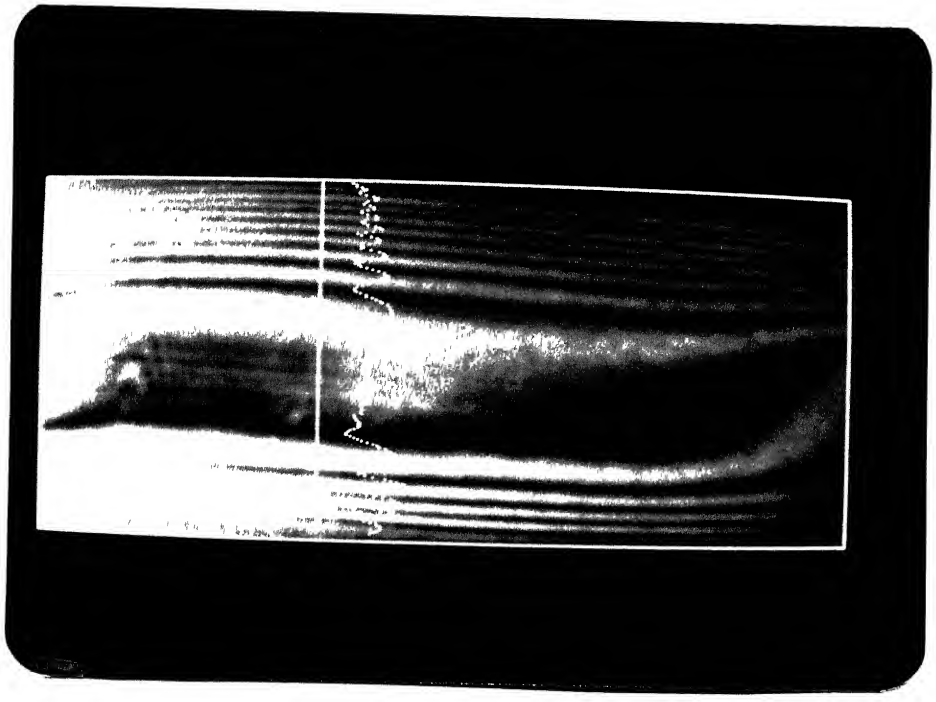

Fig (a) 0^{o} degree Projection.

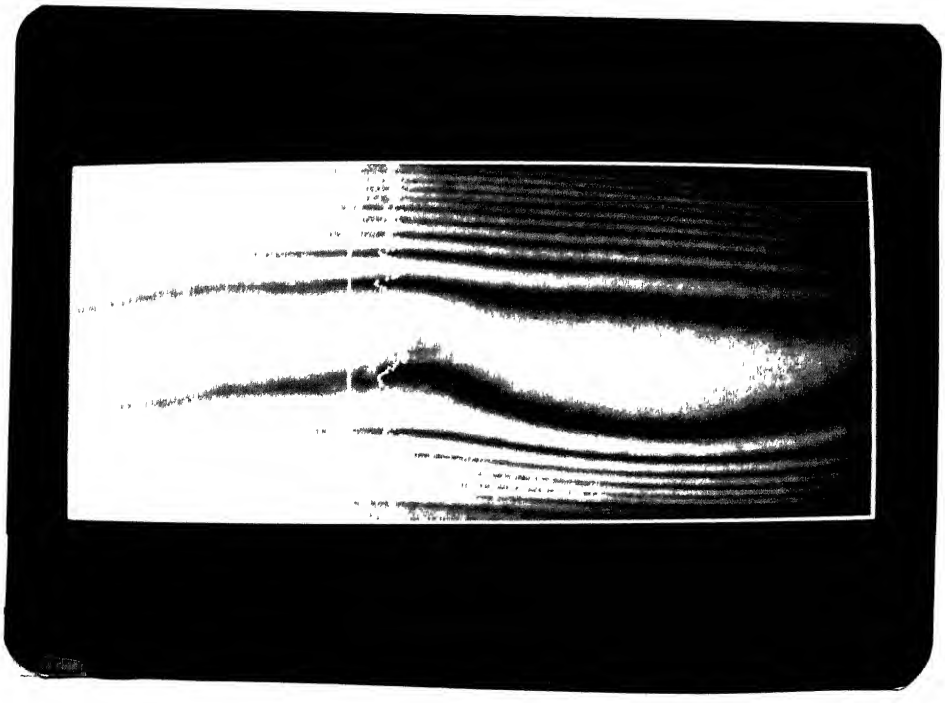

Fig (b) 90^{o} degree Projection.

Fig 5.1 Original Image with Intensity Variation.

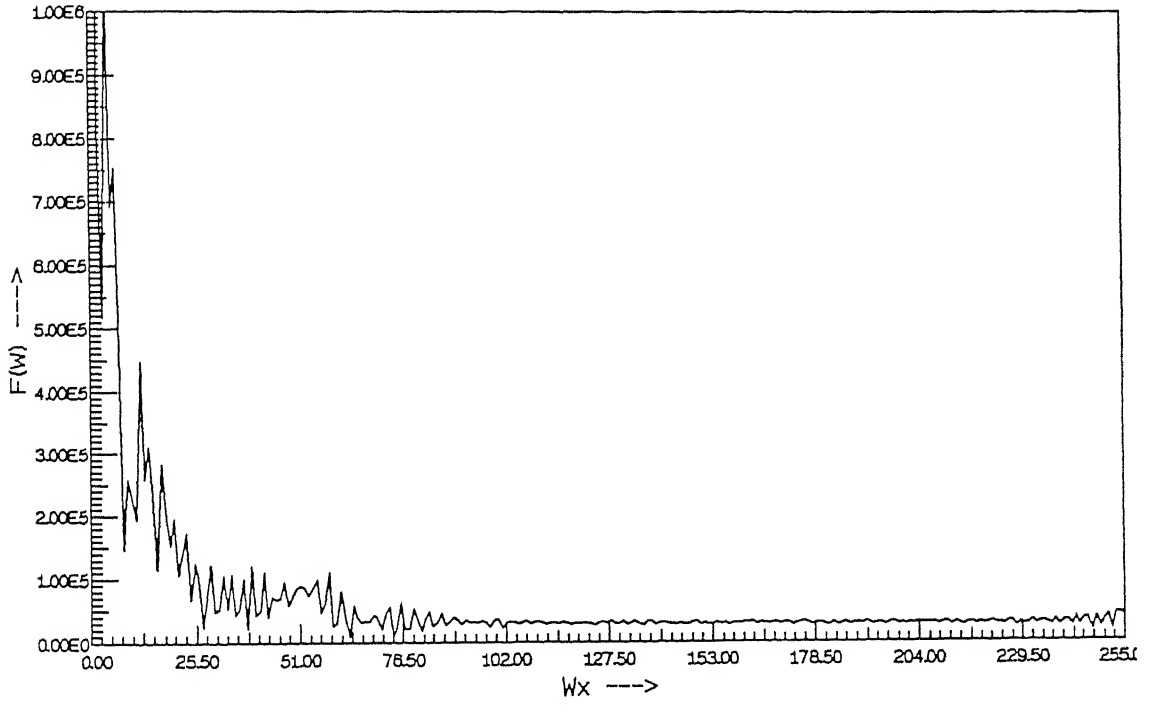

Fig 5.2 Fourier Spectrum of the Original Image corresponding to the 0^{o} degree Projection.

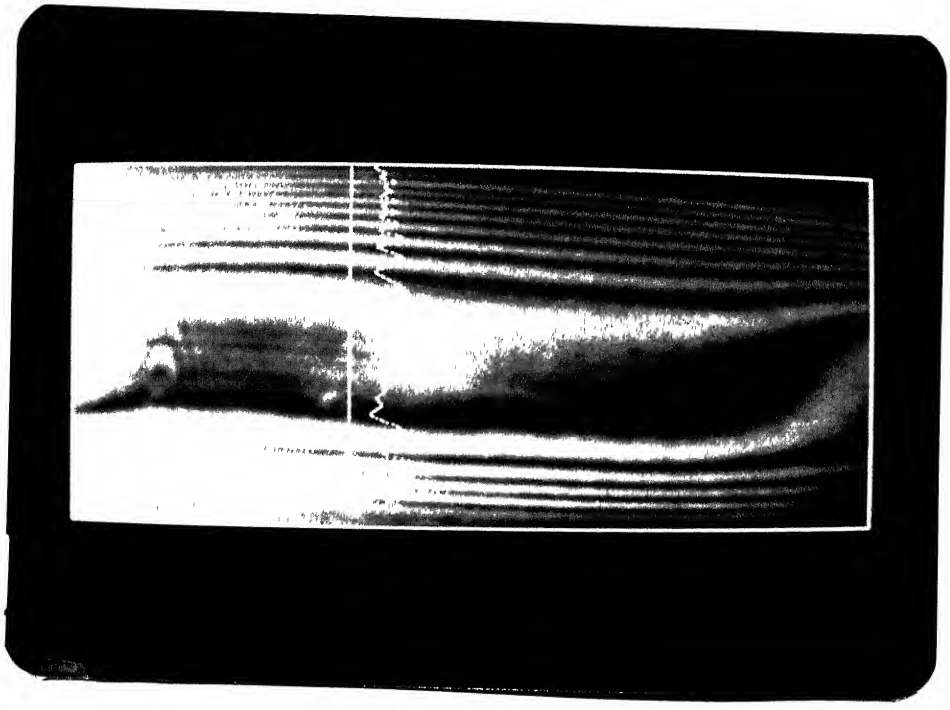

Fig (a) 0^{0} degree Projection.

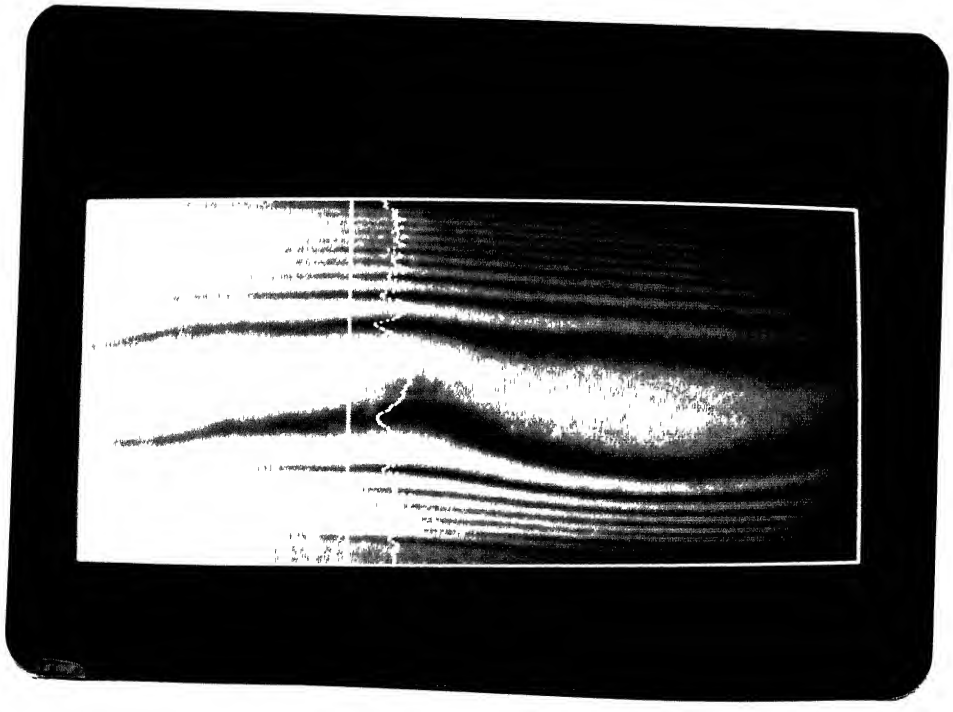

Fig (b) 90^{0} degree Projection.

Fig 5.3 Filtered Image with Intensity Variation.

Figure 5.5 show the histogram of the image before and after histogram equalization. Figure 5.6 shows the contrast improved image. Contrast improved images are thinned and are shown in Figure 5.7. Each fringe is a constant temperature line. The fringe temperatures are calculated by the method given in the section (3.2.3). Table-1 shows the fringe temperatures. The temperature on a grid is calculated using a method given in section (3.3). The grid data is used for the reconstruction of the temperature field. Temperatures are reconstructed at 21 circular rings in a X-Z plane at a time. The variation of the reconstructed temperature field for the plane Y = 0 is shown in Figure 5.8 and Figure 5.9. These two plots are for the first half (left side grid) and the second half (right side grid) respectively. They are quite similar. This implies that the flow field is axisymmetric. The plot of average Nusselt number versus radial distance for top and bottom plates are shown in Figure 5.10 and 5.11 respectively.

5.2 DIRECT MEASUREMENT :

The temperature recorded by thermocouple and the radial distance are non dimensionalised as given in section (3.4). Figure 5.12 shows the plot of non dimensional temperature versus radial distance. The nature of the variation of the temperature is similar to that available in Tritton [18]

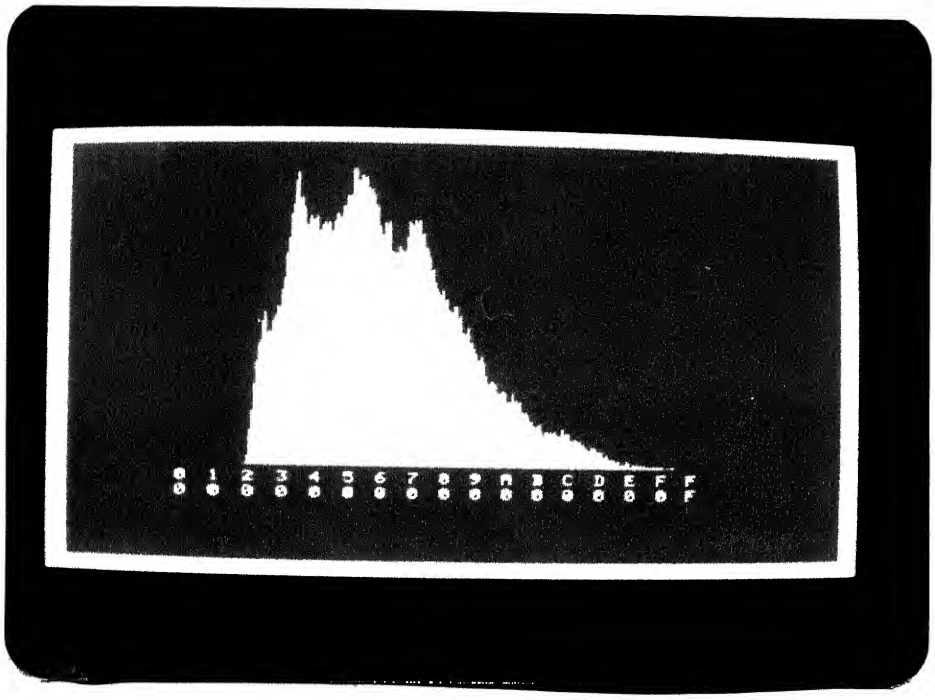

Fig 5.4 Histogram of Filtered Image Corresponding to a 0^{o} degree Projection.

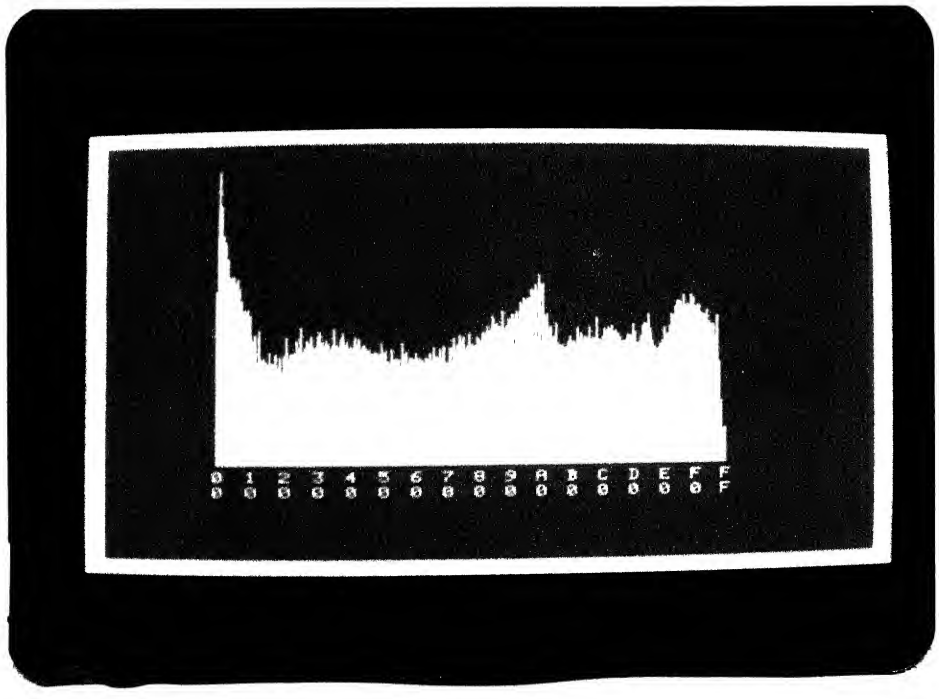

Fig 5.5 Histogram of Contrast Improved Images Corresponding to a 0^{o} degree Projection.

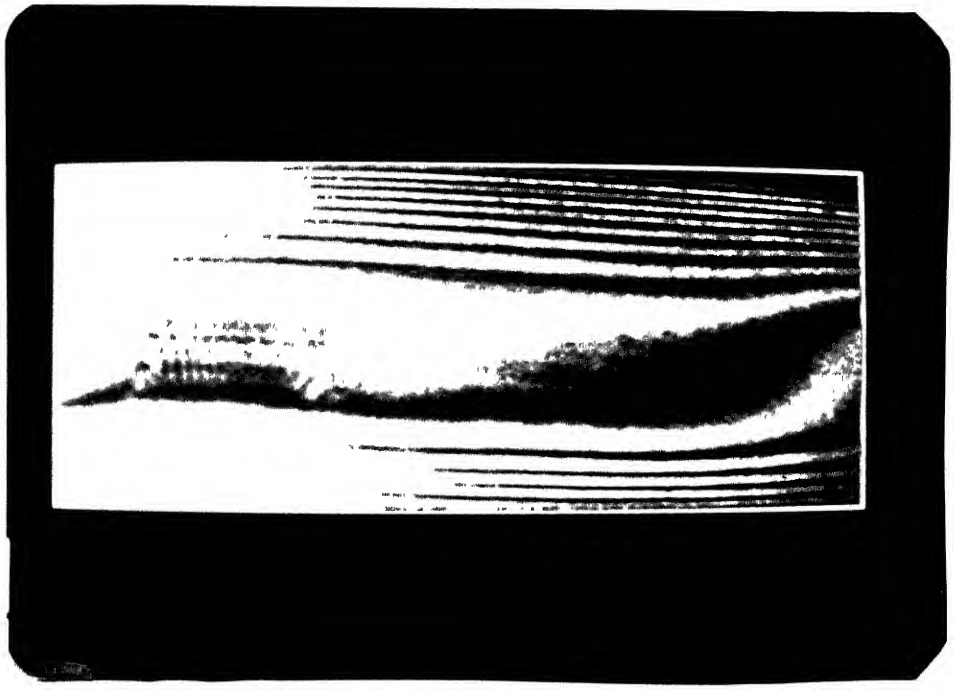

Fig 5.6 Contrast Improved Image Corresponding to a 0^{o} degree Projection.

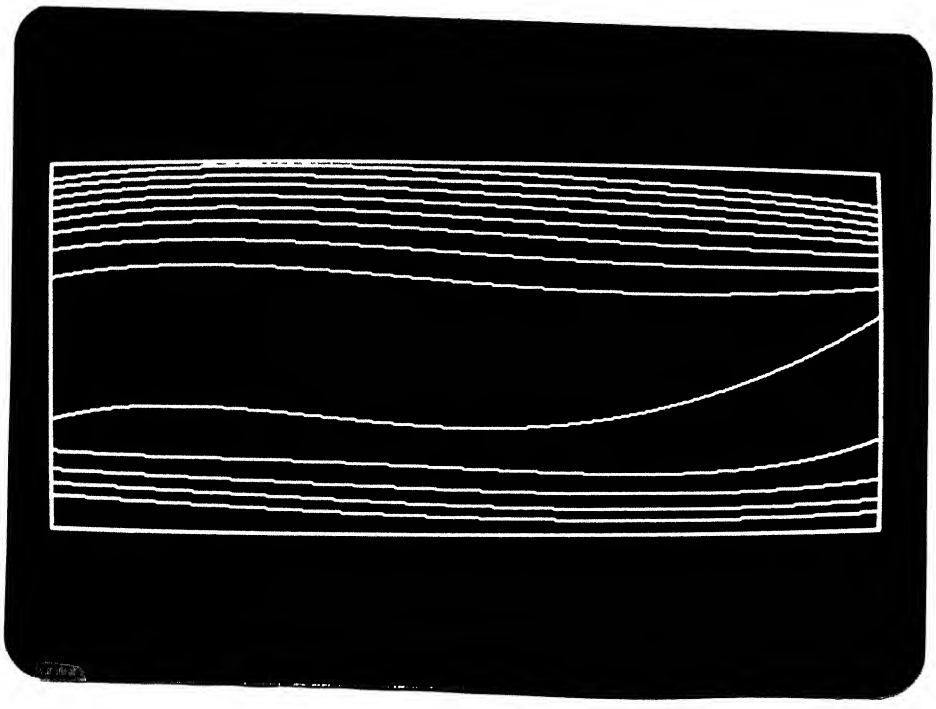

Fig (a) 0^{o} degree Projection.

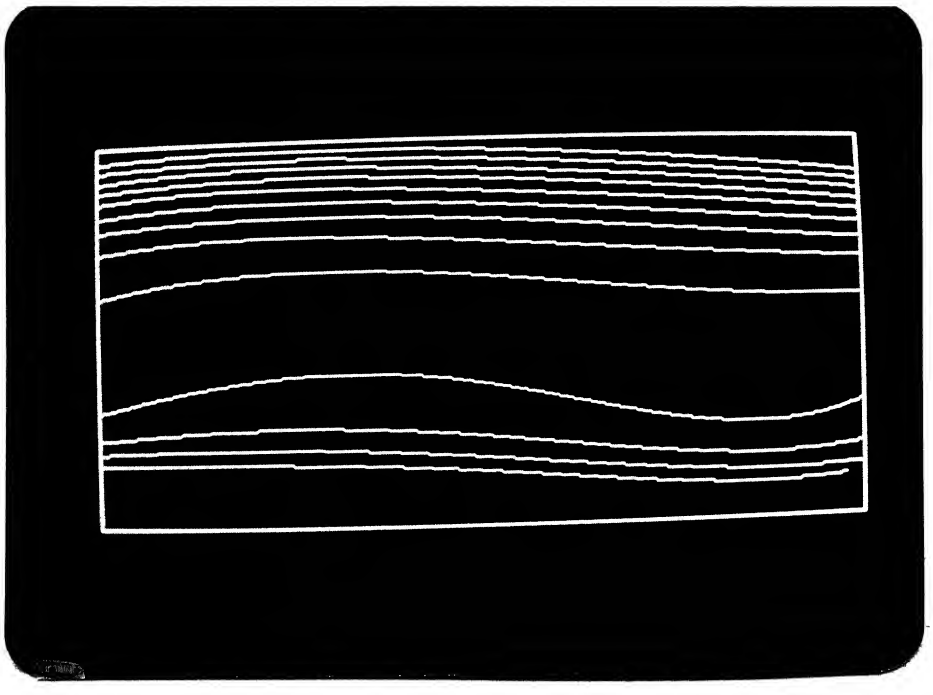

Fig (b) 90^{o} degree Projection.

Fig 5.7 Thinned Images.

Table - 1

Fringe Temperature

Fringe No. from top plate	Fringe Temperature in ^{o}C
1	23.46
2	24.36
3	25.25
4	26.15
5	27.05
6	27.95
7	28.85
8	29.74
9	30.16
10	31.05
11	31.95
12	32.85
13	33.75

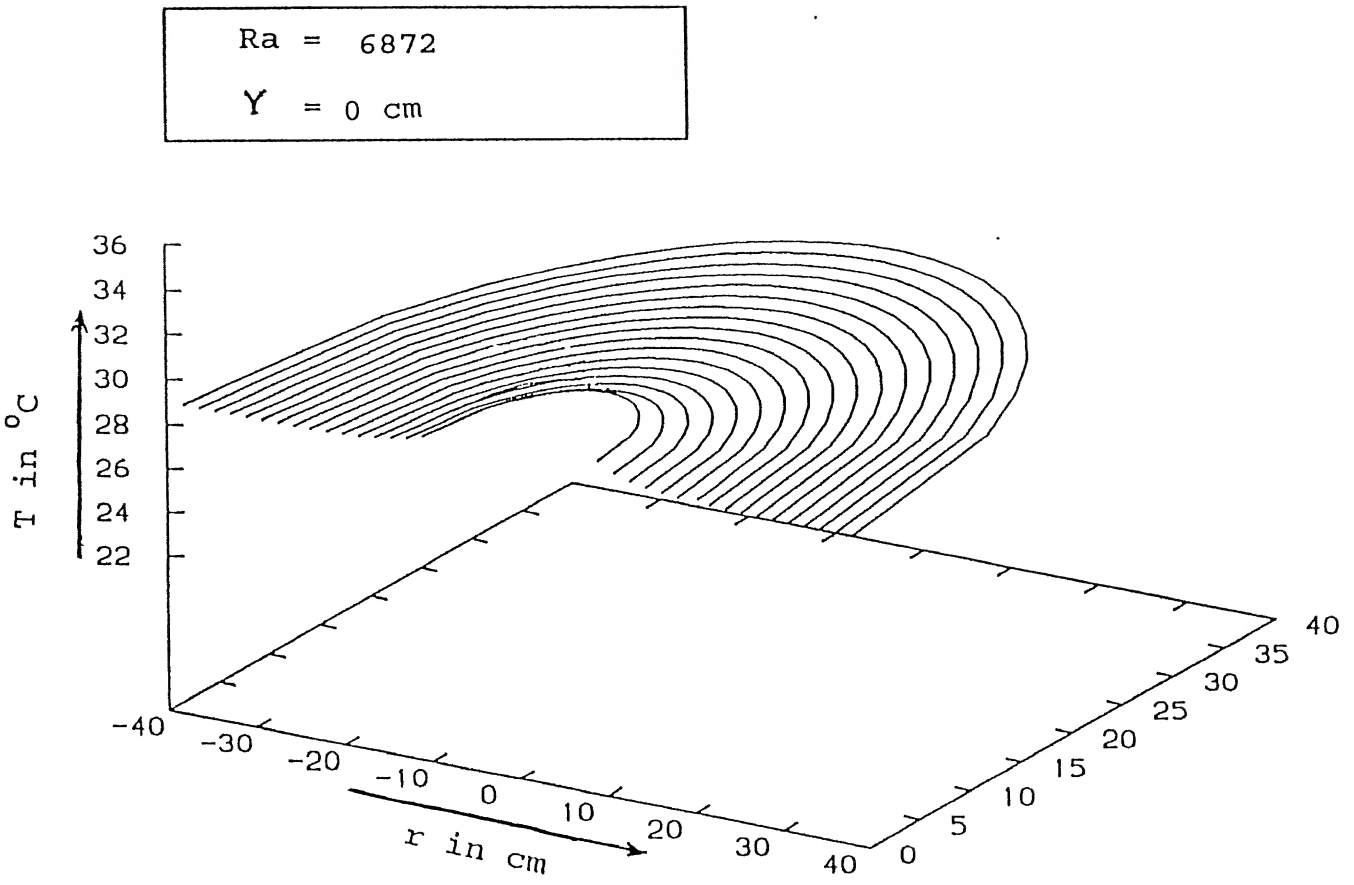

Fig 5.8 Temperature distribution of fluid at a horizontal plane, Y = 0 plane, Y = 0 (for left grid data)

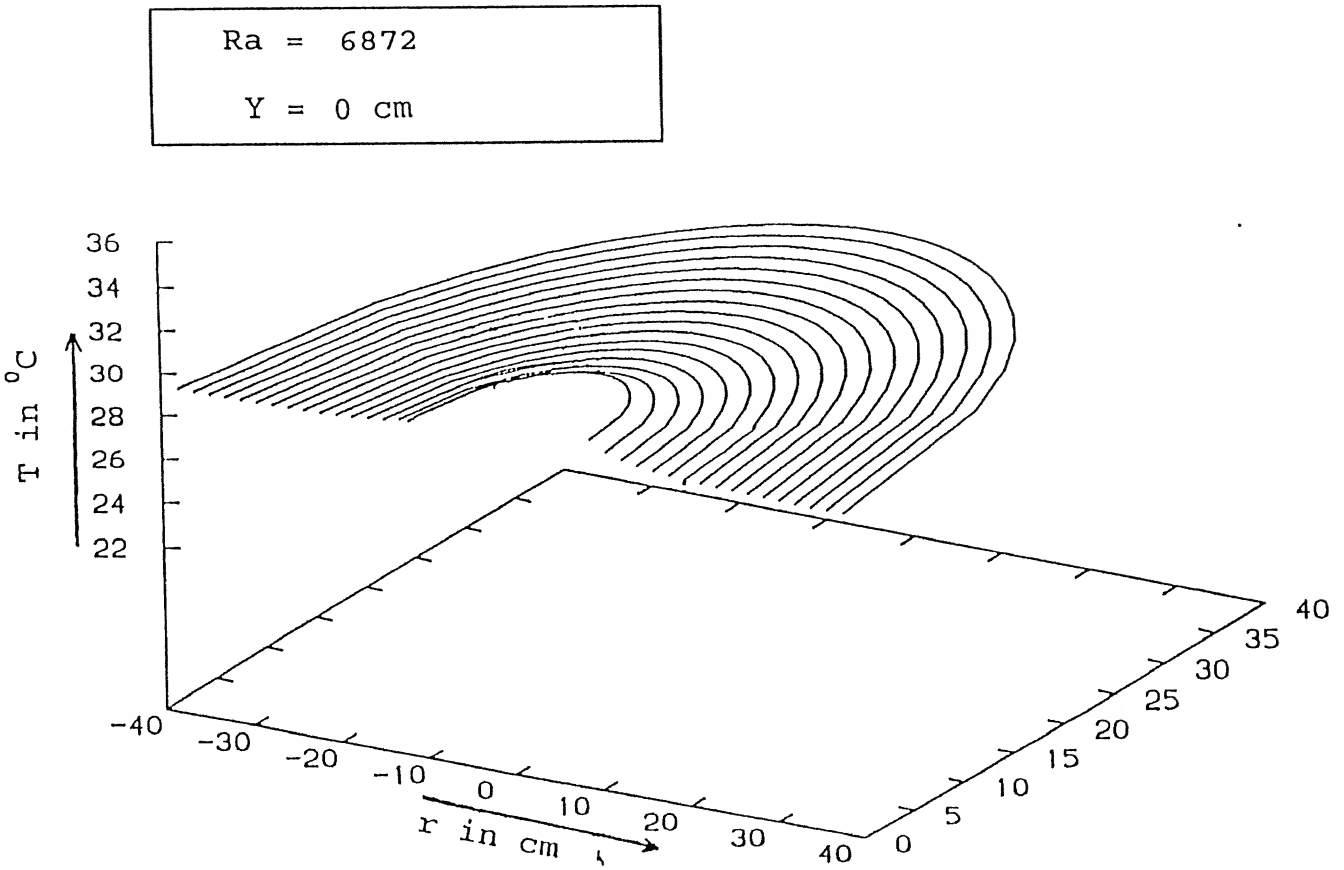

Fig 5.9 Temperature distribution of fluid at a horizontal plane, Y = 0 plane, Y = 0 (for right grid data)

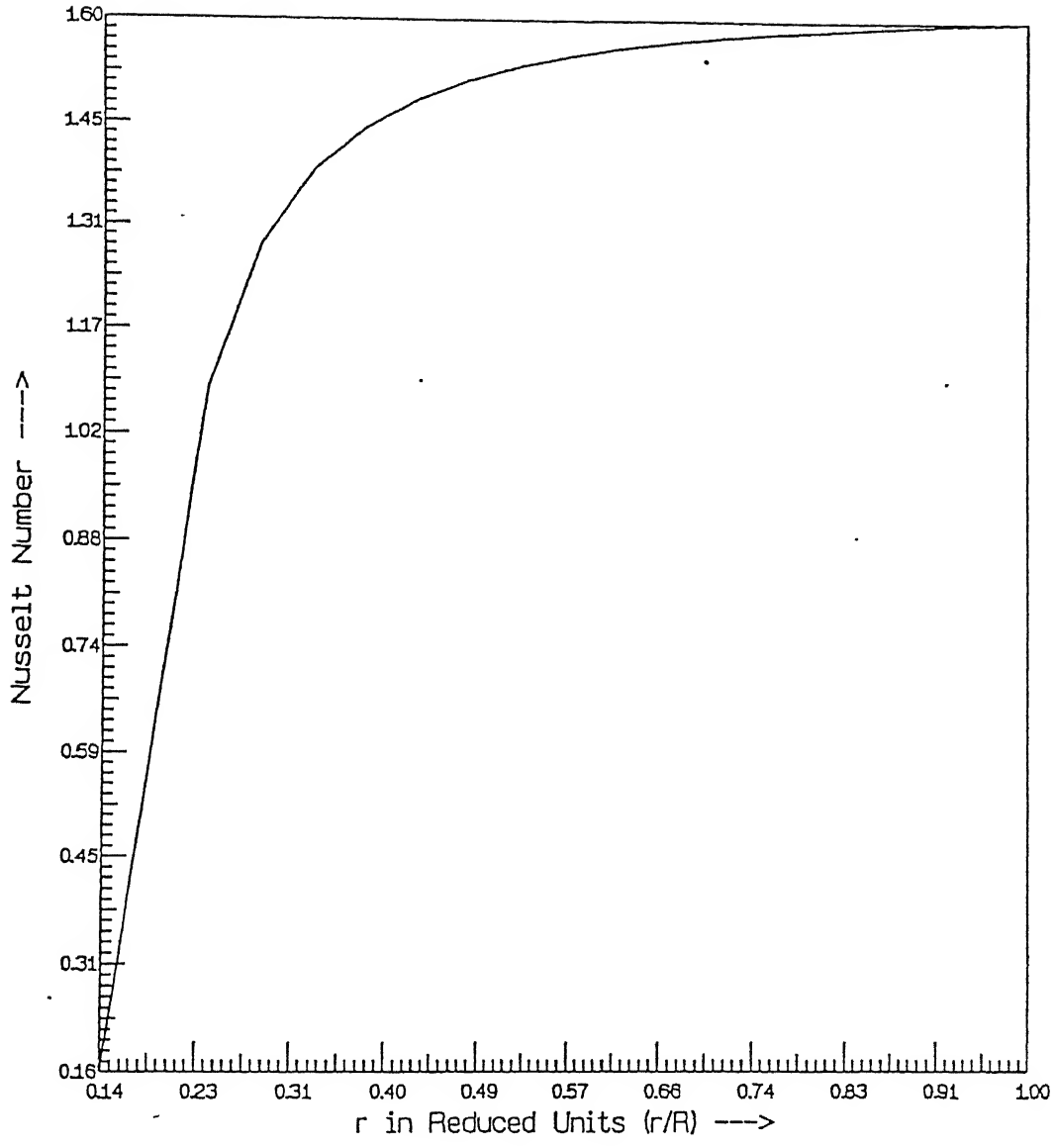

Fig 5.10 Plot of average Nu number versus radial distance at top plate.

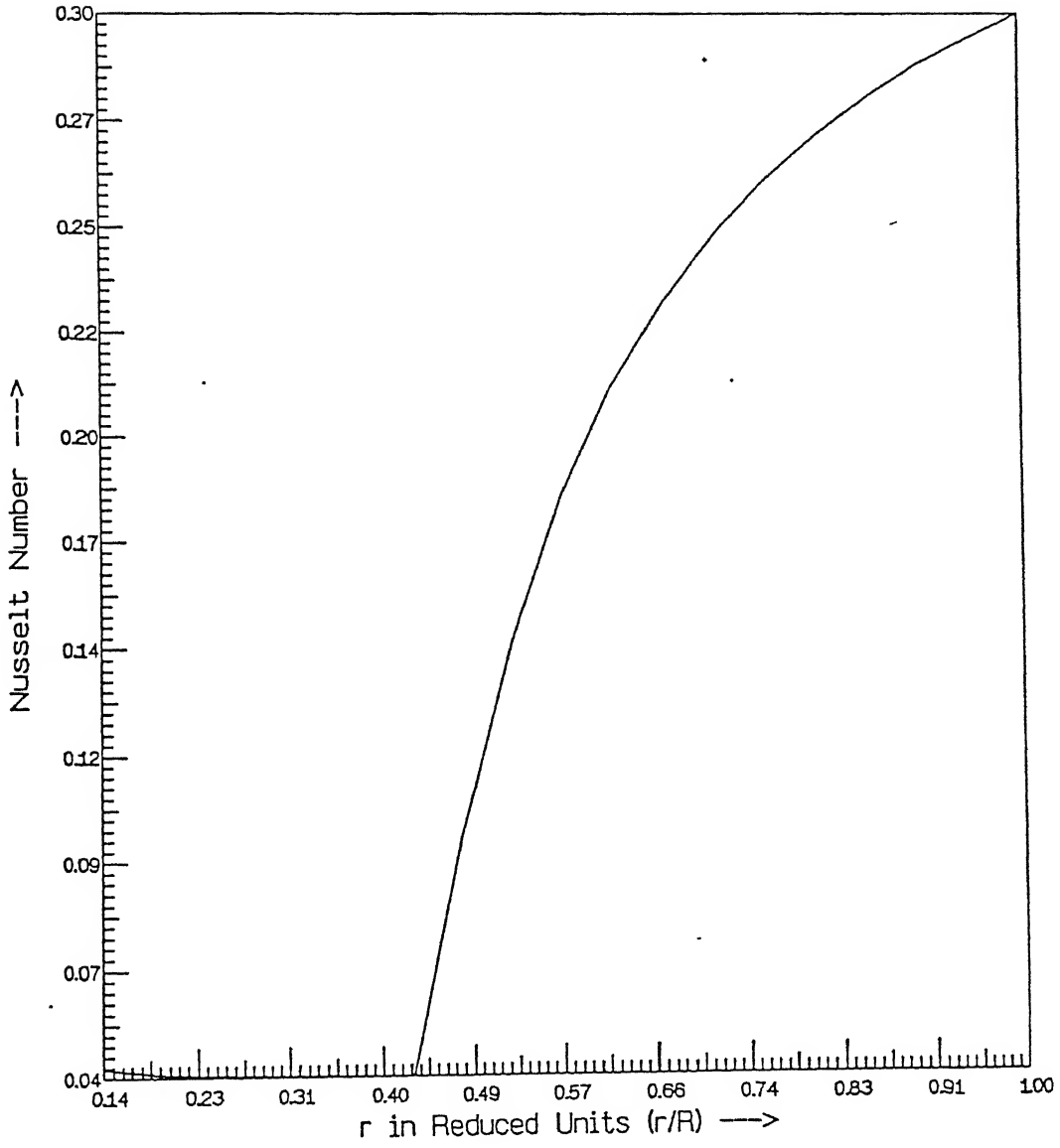

ig 5.11 Plot of average Nu number versus radial distance at bottom plate.

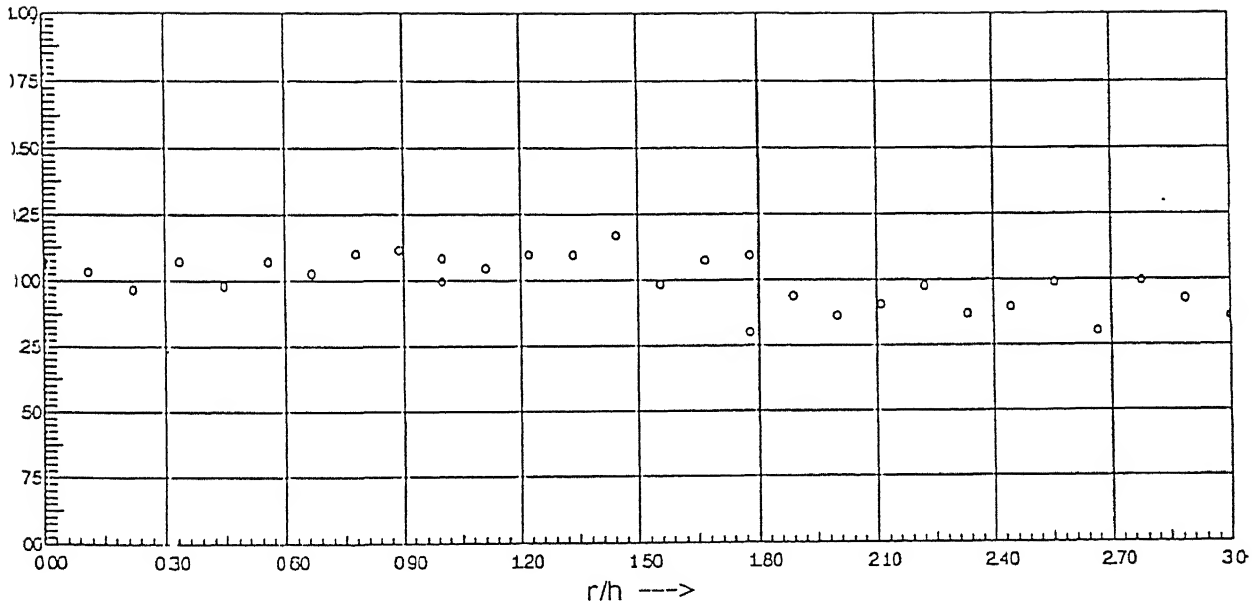

Fig 5.12 Plot of Temperature versus Radial Distance for Direct Measurement.

5.3 COMPARISON BETWEEN DIRECT AND NON-INTRUSIVE MEASUREMENT :

Table-2 shows the temperatures recorded by both direct and non-intrusive measurement. The temperature data recorded by both the methods are plotted in Figure 5.13. The magnitude of the temperatures recorded by two different methods is not same, but the trends are similar.

5.4 CONCLUSION :

Direct Measurement method gives point information while interferometric method gives both point as well as field information. In direct measurement, the roll pattern near the probe gets disturbed. This leads to an error in the temperature data. The interferometric method is non-intrusive and non-destructive.

The thickness of each circular rings taken for reconstruction is around 1.809 cm, which is of the order of the height of the cavity or the size of roll. The reconstructed temperature is the mean temperature of corresponding circular rings. Therefore the temperature variation inside a roll is not obtainable. In order to accomplish this the horizontal plane has to be divided into smaller sized circular rings. But this leads to an ill-conditioned geometric matrix. Finally the solution technique becomes extremely tricky.

Table-2

Comparison between Direct and Non-intrusive Measurements

radius r/h	Direct Measurements T in ^{o}C	Interferometric Measurements T in ^{o}C
1.000	27.4	31.673077
1.111	26.9	
1.222	26.1	
1.333	27.4	
1.444	26.2	
1.556	27.4	
1.667	26.9	
1.778	27.9	
1.889	28.1	
2.000	27.6	33.580715
2.111	27.2	
2.222	27.8	
2.333	27.8	
2.444	28.7	
2.556	26.3	
2.667	27.5	
2.778	27.7	
2.889	25.7	
3.000	24.8	32.480580
3.111	25.3	
3.222	26.2	
3.333	24.9	
3.444	25.2	
3.556	26.4	
3.667	23.9	
3.778	26.5	
3.889	25.6	
4.000	24.7	31.211583

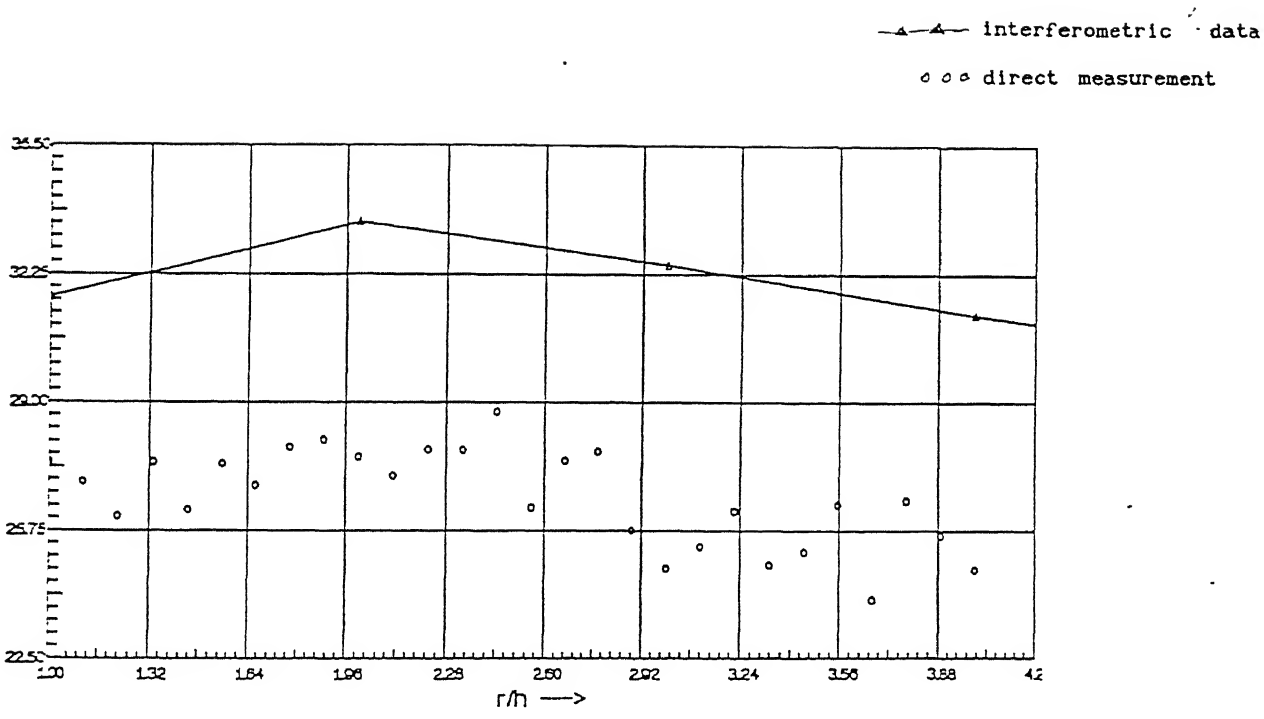

Fig 5.13 Comparison between Direct Measurement and Interferometric Measurement.

5.5 SCOPE FOR FUTURE WORK :

For further research work on present study, the number of circular rings, taken for reconstruction may be increased and a special mathematical technique has to be developed to handle ill-conditioned matrix. In order to get more accurate three dimensional temperature field using *ART algorithm*, the whole test cell can be scanned in one direction. *CSI (chord segment inversion) algorithm* can also be used for three dimensional reconstruction.

REFERENCES

1.Arroyo, M.P., and Saviron, J.M., Rayleigh-Benard convection in a small box: Spatial features and thermal dependence of the velocity field, J. Fluid Mech., Vol. 235, pp. 325-348, 1992.

2. Busse, F.H., and Clever, R.M., Instabilities of convection rolls in a fluid of moderate Prandtle number, J. Fluid Mech., Vol. 91, pp. 319-335, 1979.

3. Catton, I., The effect of insulating vertical walls on the onset of motion in a fluid heated from below,Int. J. of Heat and Mass Transfer, Vol. 15, pp 665-672, 1971.

4. Chu, T.Y., and Goldstein, R.J.,Turbulent convection in a horizontal layer of water, J. Fluid Mech., Vol. 60, part1, pp. 141-159, 1973.

5.Curry, J.H., Herring, J.R., Lonarcaric, J., and Orszag, S.A., Order and Disorder in two- and three- dimensional Benard convection, J. Fluid Mech., Vol. 147, pp. 1-38, 1984.

6. Forbes, S.J., Numerical inversion of axisymmetric interferograms, Experimental Heat Transfer, Vol. 9, pp. 49-60, 1996.

7. Gebhart B.,Jaluria y.,Mahajan R.L. and Sammakia B., *Buoyancy Induced Flow & Transport*, Hemisphere Publication Corporation.

8. Goldstein R.J. (Edited), *Fluid Mechanics Measurements*, Hemisphere Publishing Corporation, New York, 1983.

9. Gonzalez R.C. and Woods R.E., *Digital Image Processing*, Addition- Wesley Publishing Company, USA, 1993.

10. Herman G.T., *Image Reconstruction from Projections*, Academic Press, New York, 1980.

11. Kim, D.M., and Viskanta, R., Study of the effects of the wall conductance on natural convection in differently oriented square cavities, J. Fluid Mech., Vol. 144, pp. 153-176, 1984.

12.Kirchartz, K.R., and Oertel,H., Three-dimensional Thermal cellular convection in rectangular boxes, J. Fluid Mech., Vol. 192, pp.249-286, 1988.

13. Krishnamurti, R., On the transition to turbulent convection. Part 1. The transition from two- to three- dimensional flow, J. Fluid Mech., Vol. 42, part 2, pp. 295-307, 1970.

14. Mayinger F. (Edited), *Optical Measurements: Techniques and Applications*, Springer- Verlag, Berlin, 1994.

15. Michael, Y.C.,and Yang, K.T., Three-Dimensional Mach-Zehnder Interferometric Tomography of the Rayleigh-Benard Problem, Trans. of ASME, Vol. 114, pp. 622-629, 1992.

16. Muralidhar K.,Patil V.B., Kashyap R., Interferometric Study of Transient Convection in a Square Cavity, J. of Flow Visualization and Image Processing, Vol. 2, No. 4, pp 321-333, 1995.

17. Rossby, H.T., A study of Benard convection with and without rotation, J. Fluid Mech., Vol 36, pp. 309-335, 1969.

18. Tritton D.J., ***Physical fluid Dynamics***, Published by Van Nostrand Reinhold Co. Ltd., UK, 1982.